A Ratio-Difference Local Feature Contrast Method for Infrared Small Target Detection

Jinhui Han, Qiuyue Xu, Saed Moradi, Houzhang Fang, Xuye Yuan, Zhimeng Qi, and Jinyao Wan

***Abstract*— Local contrast has been proven to be effective in infrared (IR) small target detection, but existing algorithms still have some drawbacks. In this letter, a ratio-difference (RD) local feature contrast (LFC) method is proposed. First, a new nested window is designed, and the local gray contrast is selected as the features of inner and outer windows to investigate the characteristics of a local area. Then, the RD LFC is calculated. At last, a simple but useful weighting function is proposed. Experiments show that the proposed algorithm can achieve better performance in terms of detection rate and false alarm rate and has good robustness against noise.**

***Index Terms*— Infrared (IR) small target, local feature contrast (LFC), nested window, ratio-difference (RD), weighting function.**

I. Introduction

IN THE field of precise guidance, early warning, and so on, it is very important but difficult to detect infrared (IR) small target effectively and efficiently [1], because the targets are usually very small and dim and do not have enough shape or texture information. Besides, complex background, such as high brightness area, complex edges, and random noises, may bring serious interference. In addition, the target scale is usually unknown in real applications, which makes the parameter selection of the detection algorithm very difficult.

There have been many IR small target detection algorithms by now. Among them, the local contrast methods have been proven to be effective and efficient. Existing local contrast definitions can generally be divided into three types: difference-form gray contrast, ratio-form gray contrast, and ratio-difference (RD) gray contrast.

Difference-form local gray contrast algorithms, including the Laplacian of Gaussians [2], the difference of Gaussians (DoGs) [3], the Difference of Gabors [4], and the multiscale patch-based contrast measure (MPCM) [5], can eliminate high brightness background by calculating the gray difference between a current position and its surrounding benchmark. However, they cannot enhance the target, so the detection rate will not be satisfactory when the target is very dim.

Ratio-form local gray contrast algorithms, including the local contrast measure (LCM) [6], the improved LCM (ILCM) [7], and the novel LCM (NLCM) [8], take the gray ratio between the current position and its benchmark as an enhancement factor to enhance target. However, they cannot eliminate the high brightness background, so the false alarm rate will be high when the background is very complex.

The RD local gray contrast algorithms combine the ratio-form and difference-form local gray contrast as a whole. For example, the relative LCM (RLCM) [9] is a typical RD local gray contrast algorithm, and it was also used with the multidirectional two-dimensional least mean square (MDTDLMS) [10] or the multiscale Gaussian filter [11].

In addition to the three basic types of local contrast algorithms, there are some new improvements in recent years.

1) Using features instead of gray values to calculate local feature contrast (LFC). For example, the variance difference (VAR-DIFF) algorithm [12] selected the variances of the central layer and surrounding layer of the window as features, Xiong *et al.* [13] selected the gradients as features, and so on.
2) Using more information as weighting functions to improve detection performance further. For example, the weighted local difference measure (WLDM) algorithm [14] selected the local entropy as a weighting function, the homogeneity-weighted LCM algorithm [15] used the local homogeneity as a weighting function, and so on.

However, there are still some drawbacks in the existing algorithms. First, feature can describe the characteristics of a local area more exactly than gray, but the features selected in the existing algorithms are too simple, and they do not work well when the background is complex. Also, RD operation can enhance target and suppress complex background simultaneously, but it has not been researched in the field of LFC. Moreover, weighting function is a good method to improve detection performance, but the existing weighting functions are usually too complex.

In this letter, an RD LFC method is proposed. The main contributions can be summarized as follows: 1) a new nested window is proposed, and the local gray contrast information, which has been proven effective for IR small target detection, is selected as features of the inner and outer windows; 2) some newest ideas of local gray contrast, for example, the RD joint operation and so on, are adopted to the calculation of LFC; and 3) a simple but useful weighting function is proposed.

II. Proposed Algorithm

The flowchart of the proposed algorithm is shown in Fig. 1.

A. Design of the New Nested Window

Fig. 2 shows the new nested window designed in this letter. It consists of 9 × 9 blocks (each block is 3 × 3 pixels) and can be divided into an inner window and eight outer windows. The inner window is constructed by 5 × 5 blocks,

Manuscript received July 23, 2021; revised October 9, 2021; accepted October 25, 2021. Date of publication March 10, 2022; date of current version April 20, 2022. This work was supported in part by the National Natural Science Foundation of China under Grant 61802455; in part by the Foundation of China Scholarship Council under Grant 202108410232; in part by the Foundation of the Science and Technology Department of Henan Province under Grant 192102210089, Grant 222102210077, and Grant 222102320370; and in part by the Foundation of the Zhoukou Science and Technology Bureau under Grant 2021GG01001. *(Corresponding author: Jinhui Han.)*

Jinhui Han, Qiuyue Xu, Xuye Yuan, Zhimeng Qi, and Jinyao Wan are with the College of Physics and Telecommunication Engineering, Zhoukou Normal University, Zhoukou 466001, China (e-mail: hanjinhui@zknu.edu.cn).

Saed Moradi is with the Department of Electrical Engineering, Faculty of Engineering, University of Isfahan, Isfahan 817746-73441, Iran.

Houzhang Fang is with the School of Computer Science and Technology, Xidian University, Xi'an 710071, China.

Digital Object Identifier 10.1109/LGRS.2022.3157674

1558-0571 © 2022 IEEE. Personal use is permitted, but republication/redistribution requires IEEE permission.
See https://www.ieee.org/publications/rights/index.html for more information.

Authorized licensed use limited to: XIDIAN UNIVERSITY. Downloaded on August 13,2026 at 11:09:15 UTC from IEEE Xplore. Restrictions apply.

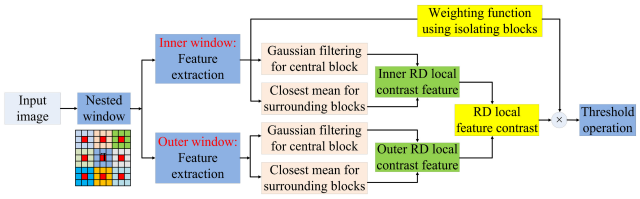


Fig. 1. Flowchart of the proposed algorithm.

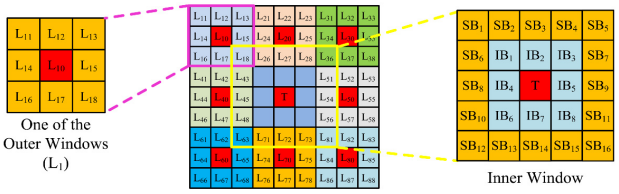


Fig. 2. New nested window used in the proposed algorithm.

including a central block T, eight isolating blocks IB_1–IB_8 (they can separate the target from its surrounding background, so it will not need to adjust the window size to detect targets with unknown scale), and 16 surrounding blocks SB_1–SB_{16}. The nth outer window L_n has a central block L_{n0} and eight surrounding blocks L_{n1}–L_{n8}. Note that the inner and outer windows are overlapped with each other.

B. Feature Extraction for the Inner and Outer Windows

Place the nested window on the image and slide it from left to right and top to bottom; at each pixel, the features of the inner and outer windows are extracted first. In this letter, considering that local gray contrast is a good method to describe local image information, we have decided to choose local gray contrast of the inner and outer windows as their features, respectively.

1) Feature Extraction of the Inner Window: To deal with complex background more effectively, we will apply a Gaussian filtering on the central block T and use the closest mean principle to select the background benchmark between SB_1 and SB_{16}, and finally, we will calculate the RD local gray contrast (i.e., the inner feature) between them.

a) Gaussian filtering for the central block T: According to the theory of the matched filter, when data are processed using the filtering method, the SNR will be improved best when the shape of the filter template is the same as the signal's shape [16]. Considering that a true small target is very similar to a Gaussian function in shape, a 3×3 Gaussian template $G = [1\ 2\ 1;\ 2\ 4\ 2;\ 1\ 2\ 1]/16$ is applied on the central block T, and, at the location (i, j), the Gaussian filtering result IG_{in} is

$$IG_{in}(i,j) = \sum_{p=-1}^{+1}\sum_{q=-1}^{+1}[G(p,q)\cdot T(i+p, j+q)] \quad (1)$$

where T is the central block and G is the Gaussian template.

b) Closest mean principle for surrounding blocks: There are 16 surrounding blocks in the inner window. In the existing algorithms, people usually choose the largest one as the benchmark for contrast calculation to suppress edges. However, when a target is located near a high brightness background, the target will be missed. To solve this problem, the surrounding block with the closest mean gray value to the central block will be selected as the benchmark in this letter

$$B_{in}(i,j) = \arg\min_{m_{SBx}} |m_{SBx} - IG_{in}(i,j)|, \quad x = 1, 2, \ldots, 16 \quad (2)$$

where m_{SBx} is the mean gray value of the xth surrounding block and B_{in} is the final benchmark for the inner window.

c) RD local gray contrast for the inner window: The RD local gray contrast information RD_{in} is calculated as

$$RD_{in}(i,j) = \frac{IG_{in}(i,j)}{\max[B_{in}(i,j), \xi]} IG_{in}(i,j) - IG_{in}(i,j) \quad (3)$$

where ξ is a small value to avoid a zero denominator, in our approach, for an 8-bit image, and ξ is set to 5.

2) Feature Extraction of Outer Windows: For the nth outer window, similar to the inner window, the RD local gray contrast RD_{outn} is defined as

$$IG_{outn}(i,j) = \sum_{p=-1}^{+1}\sum_{q=-1}^{+1}[G(p,q)\cdot L_{n0}(i+p, j+q)] \quad (4)$$

$$B_{outn}(i,j) = \arg\min_{m_{Lnx}} |m_{Lnx} - IG_{outn}(i,j)|, \quad x = 1, 2, \ldots, 8 \quad (5)$$

$$RD_{outn}(i,j) = \frac{IG_{outn}(i,j)}{\max[B_{outn}(i,j), \xi]} IG_{outn}(i,j) - IG_{outn}(i,j) \quad (6)$$

where L_{n0} is the central block of the nth outer window, IG_{outn} is the filtering results of the central block of the nth outer window, m_{Lnx} is the mean gray value of L_{nx}, and B_{outn} is the benchmark for the nth outer window.

The final outer feature RD_{out} will be

$$RD_{out}(i,j) = \arg\min_{RD_{outn}} |RD_{outn}(i,j) - RD_{in}(i,j)| \quad n = 1, 2, \ldots, 8. \quad (7)$$

C. Calculation of RD LFC

The RD LFC of pixel (i, j) will be calculated between the inner feature RD_{in} and the outer feature RD_{out}

$$LFC(i,j) = \left\{\frac{RD_{in}(i,j)}{\max[RD_{out}(i,j), \xi]} RD_{in}(i,j) - RD_{in}(i,j)\right\}^2. \quad (8)$$

The square operation is to avoid obtaining a negative value.

D. Definition of the Weighting Function

Considering that a true target usually attenuates from center to surroundings, a simple but useful weighting function is designed to further suppress background clutter: the weighting parameter $W(i, j)$ will be set to 1 only if the maximum gray value of the central block T is larger than the mean gray value of any isolating blocks (IB_1–IB_8), or else $W(i, j)$ will be set to 0. The final saliency map (SM) will be defined as the product of LFC and the weighting function, that is

$$SM(i,j) = LFC(i,j)\cdot W(i,j). \quad (9)$$

III. Discussions and Threshold Operation

A. Detection Ability Analysis

It is necessary to discuss different cases when (i, j) is true target center, flat background (including high brightness background), random noise pixel, and background edge [see Fig. 3(a)–(d)]. The target is shown as a yellow circle in Fig. 3(a).

1) When (i, j) is the true target center. Suppose the maximum gray of the target is P, and the surrounding background is $Q(P > Q)$. For the inner window, $IG_{in} \approx P$, $B_{in} \approx Q$, so $RD_{in} > 0$. For the outer

Authorized licensed use limited to: XIDIAN UNIVERSITY. Downloaded on August 13,2026 at 11:09:15 UTC from IEEE Xplore. Restrictions apply.

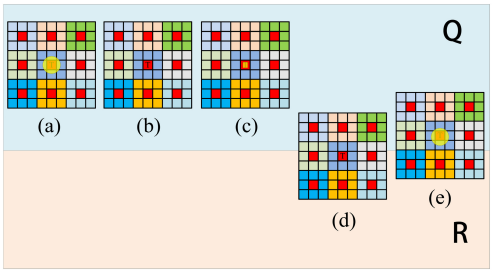


Fig. 3. Different cases for different types of pixels.

windows, since a true target usually emerges in a small flat area, $\mathrm{IG}_{\mathrm{out}n} \approx B_{\mathrm{out}n} \approx Q$, so $\mathrm{RD}_{\mathrm{out}n} \approx \mathrm{RD}_{\mathrm{out}} \approx 0$. For the weighting function, since a target usually attenuates from center to the surroundings, $W(i, j) = 1$. Finally, $\mathrm{SM}(i, j) > 0$.

2) When (i, j) is a flat background. Suppose the background gray value is Q. For the inner window, $\mathrm{IG}_{\mathrm{in}} \approx B_{\mathrm{in}} \approx Q$, so $\mathrm{RD}_{\mathrm{in}} \approx 0$. For the outer windows, $\mathrm{IG}_{\mathrm{out}n} \approx B_{\mathrm{out}n} \approx Q$, so $\mathrm{RD}_{\mathrm{out}n} \approx \mathrm{RD}_{\mathrm{out}} \approx 0$. For the weighting function, since the background is flat, $W(i, j) = 0$. Finally, $\mathrm{SM}(i, j) \approx 0$.
3) When (i, j) is a random noise pixel [the yellow square in Fig. 3(c)]. Suppose the noise gray value is close to the maximum target value and it is P, the background is Q, the analysis will be similar to the true target and then $\mathrm{SM}(i, j) > 0$. However, considering that a random noise usually emerges as a single pixel, it can be easy to deduce that its SM will be smaller than the SM of a true target, so it will not disturb the target detection.
4) When (i, j) is near a background edge and it is on the brighter side. Suppose the gray value of each side is Q and R, respectively, and $R > Q$. For the inner window, $\mathrm{IG}_{\mathrm{in}} \approx B_{\mathrm{in}} \approx R$, so $\mathrm{RD}_{\mathrm{in}} \approx 0$. For the outer windows, when an outer window is totally located on one side, its feature $\mathrm{RD}_{\mathrm{out}n} \approx 0$. Therefore, $\mathrm{RD}_{\mathrm{out}} \approx 0$ too. For the weighting function, since there are some isolating blocks that have the same gray value as that of the central block T, $W(i, j) = 0$. Finally, $\mathrm{SM}(i, j) \approx 0$. (On the darker side, similar conclusions can be obtained.)

There is a special case when a target is located near a high brightness background [see Fig. 3(e)]. Suppose the maximum gray value of the target is P, the surrounding background is Q, the background on the other side is R, and $R \gg P > Q$. Then, for the inner window, $\mathrm{IG}_{\mathrm{in}} \approx P$, the mean gray value of some surrounding blocks will be close to Q, and other surrounding blocks will be close to R, so $B_{\mathrm{in}} \approx Q$. Therefore, $\mathrm{RD}_{\mathrm{in}} > 0$. For the outer windows, some outer windows are located in the flat background, others are located near a background edge, and according to the previous analysis, their features will all be close to 0, so $\mathrm{RD}_{\mathrm{out}} \approx 0$ too. For the weighting function, similar to the case of a true target, $W(i, j) = 1$. Finally, $\mathrm{SM}(i, j) > 0$, which means that the target can still be detected.

B. Threshold Operation

In SM, the target will be the most salient, so a threshold operation will be adopted to extract the target. First, the SM is normalized to 0–1, then the threshold TH will be defined as

$$\mathrm{TH} = \mu + k \cdot \mathrm{std} \tag{10}$$

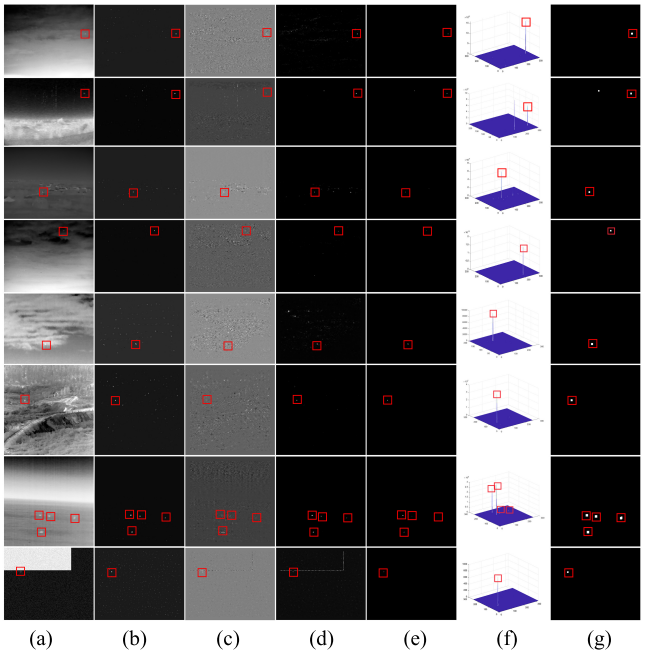


Fig. 4. Detection results for the eight sequences. (a) Raw image. (b) Feature of the inner window. (c) Feature of the outer window. (d) RD LFC. (e) SM after weighting. (f) 3-D show of (e). (g) Final output.

where μ and std are the mean and standard deviation of SM, respectively, and k is a given factor. Our experiments show that 30–100 will be suitable for single-target detection.

Using TH to binarize SM, the pixels larger than TH are marked as 1, and the pixels smaller than TH are marked as 0. Finally, each connected area with a value of 1 is regarded as a detected target (in order to reduce clutter, a dilation is suggested before outputting the target).

IV. Experimental Results and Comparisons

A. Experimental Results Using the Proposed Algorithm

To verify the effectiveness of the proposed algorithm, eight sequences (totally 1470 frames) were used for tests, including seven real sequences with different types and sizes of targets, and one simulated sequence containing a small target located near a high brightness background. All the experiments were conducted in MATLAB R2016b on a PC with a 2.6-GHz Intel i5-8250 CPU and 8-GB RAM.

Fig. 4 gives the detection results for the eight sequences. From Fig. 4, it can be seen that: 1) in the raw image, the target is usually small and dim, and the background is very complex; 2) in the feature of the inner window, target becomes obvious, but there are some complex background residuals; 3) in the feature of the outer window, there are some complex background residuals too (for example, the background edges); 4) after the RD LFC calculation, target becomes very salient, and the complex background is suppressed more successfully; 5) after the weighting operation, almost all of the complex background is suppressed, and target becomes the most salient; and 6) in the final detection results, all of the true targets are output successfully, with only one false alarm in Sequence 2. It should be noticed that the proposed algorithm can detect different sizes of targets and targets that are near high brightness background.

Authorized licensed use limited to: XIDIAN UNIVERSITY. Downloaded on August 13,2026 at 11:09:15 UTC from IEEE Xplore. Restrictions apply.

TABLE I

SCRG OF DIFFERENT ALGORITHMS IN THE SAMPLE FRAMES OF THE EIGHT SEQUENCES

Seq	Target	DoG	MPCM	ILCM	NLCM	RLCM	MDTDLMS	WLDM	VAR-DIFF	DLCM	Proposed
1	1	9.3889	9.5588	17.0028	30.2405	17.6701	101.2353	45.1927	198.1542	444.8878	**546.1672**
2	1	6.2885	7.6446	7.2875	10.1899	15.7705	51.2914	18.5764	92.1675	129.7833	**162.3442**
3	1	0.5052	2.0665	1.9404	1.6612	1.5181	3.6358	19.0926	7.9416	14.8091	**20.3693**
4	1	13.9985	8.3706	46.9499	44.1210	20.1072	134.0081	96.6349	81.0621	346.6128	**447.1544**
5	1	1.9132	2.9264	6.0963	5.5267	2.5565	12.6830	7.8443	44.2458	**58.3362**	49.8844
6	1	1.1451	1.8120	4.4645	5.5739	3.8397	12.7133	6.6120	21.4419	49.7060	**53.6952**
7	1	8.4327	8.3807	4.4035	0.3048	8.1419	35.3682	38.6412	48.5450	**144.0714**	70.7062
	2	6.0860	6.4653	14.0724	7.6629	7.0714	44.1577	34.1497	22.5104	**115.3426**	109.7767
	3	5.9508	8.9205	3.5529	2.8184	6.5915	46.3951	19.3874	6.8973	**72.3783**	21.7840
	4	5.3314	6.9744	3.4226	0.0654	6.5919	37.2507	18.1551	4.4662	**60.5618**	5.1352
8	1	1.1238	2.6805	2.0236	2.6389	7.1062	0.6750	0.7468	1.3597	0.0000	**129.7631**

TABLE II

BSF OF DIFFERENT ALGORITHMS IN THE SAMPLE FRAMES OF THE EIGHT SEQUENCES

Seq	DoG	MPCM	ILCM	NLCM	RLCM	MDTDLMS	WLDM	VAR-DIFF	DLCM	Proposed
1	7.1437	0.0299	94.5928	0.1103	15.3719	1.8704E5	39.7668	3.8129E-9	8.1327E5	**9.9840E5**
2	2.1241	0.5767	3.9468	1.4121	6.1397	3.4236E3	681.6723	2.8000E-3	6.8681E3	**1.0426E4**
3	0.4814	0.1368	9.1742	0.0344	2.1982	4.2422E3	16.5951	7.4519E-9	1.7194E4	**2.3649E4**
4	5.7067	0.0192	46.3694	0.0220	15.1353	3.8940E5	22.8578	5.0430E-10	1.0026E6	**1.2935E6**
5	0.7430	0.3002	17.4796	1.0426	2.7740	660.7865	112.1502	0.0119	**3.0081E3**	2.5722E3
6	0.4502	0.1257	6.9512	0.0567	2.2033	1.8657E3	37.5616	1.3918E-5	7.2556E3	**7.8379E3**
7	2.1606	0.7421	29.8661	0.6584	5.2646	2.3261E3	536.9486	1.6158E-4	**6.0830E3**	5.7417E3
8	0.6452	0.4048	16.4929	0.4706	4.1212	690.4329	44.9468	2.9000E-3	6.7822E3	**9.2544E3**

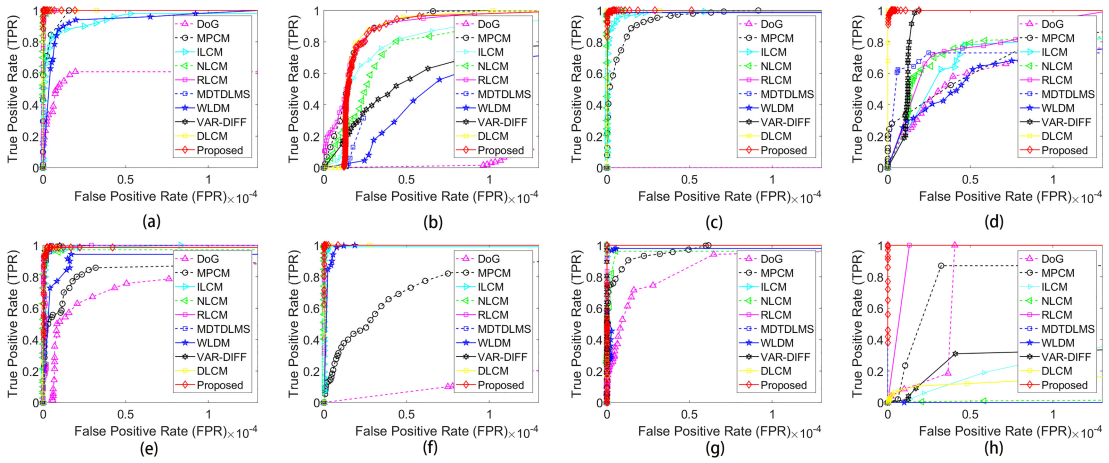


Fig. 5. ROC curves in the eight sequences. (a)–(h) Sequences 1–8.

B. Comparisons With Some State-of-the-Art Algorithms

To illustrate the advantages of the proposed algorithm further, nine existing algorithms were selected as baseline for comparisons, including DoG [3], MPCM [5], ILCM [7], NLCM [8], RLCM [9], MDTDLMS [10], WLDM [14], VAR-DIFF [12], and the double-layer LCM (DLCM) [17]. The parameter settings in the baseline algorithms are the same with the values recommended by the authors.

First, Tables I and II give the signal-clutter ratio gain (SCRG) and background suppression factor (BSF) of different algorithms, respectively. The SCRG and BSF are defined as

$$\text{SCRG} = \frac{\text{SCR}_{\text{out}}}{\text{SCR}_{\text{in}}}, \quad \text{BSF} = \frac{\sigma_{\text{in}}}{\sigma_{\text{out}}} \tag{11}$$

where SCR_{in} and SCR_{out} are the signal-clutter ratio of the raw IR image and the SM, respectively. σ_{in} and σ_{out} are the standard deviation of the raw IR image and the SM, respectively.

Then, for the eight sequences, the receiver operating characteristic (ROC) curve is applied to further illustrate the advantage of the proposed algorithm, as shown in Fig. 5. Here, the true positive rate (TPR) is defined as the ratio of the number of detected true targets and the total number of true targets, and the false positive rate (FPR) is defined as the ratio of the number of detected false targets and the total number of pixels in the whole image.

From Tables I and II and Fig. 5, it can be seen that:

Both DoG and MPCM are difference-form local gray contrast algorithms, and their performance is not very good sometimes. For example, in Sequences 3–8.

Both ILCM and NLCM are ratio-form local gray contrast algorithms. However, in Sequences 1, 2, 4, and 8, their performance is not satisfactory.

Both RLCM and MDTDLMS are RD local gray contrast algorithms, and their performance is significantly better than

Authorized licensed use limited to: XIDIAN UNIVERSITY. Downloaded on August 13,2026 at 11:09:15 UTC from IEEE Xplore. Restrictions apply.

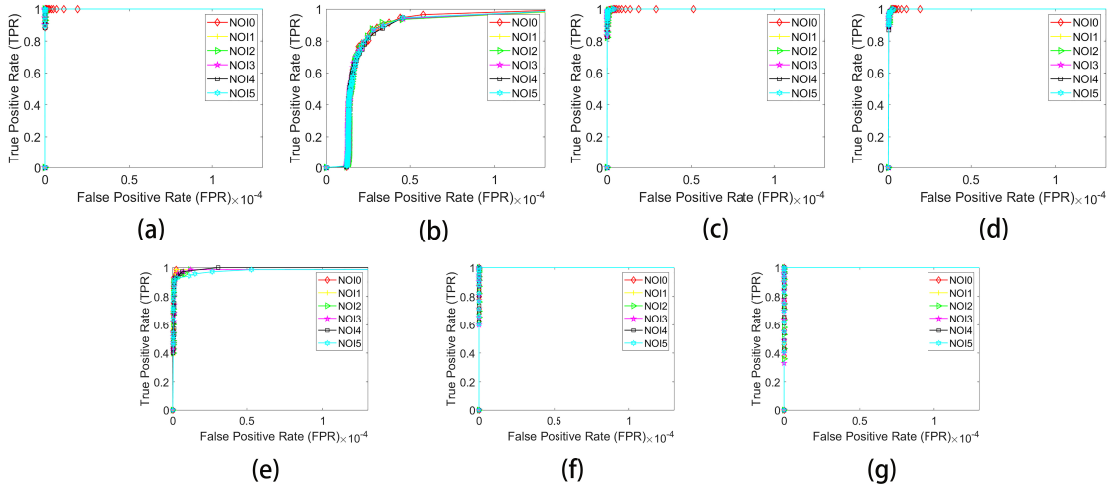


Fig. 6. ROC curves in the seven real sequence under noise. (a)–(g) Sequences 1–7.

that of some previous methods. However, in Sequence 4, their performance is not good enough.

WLDM is a weighted local contrast algorithm, but only uses a difference-form local gray contrast, so its performance is not very good sometimes, for example, in Sequences 1, 2, 4, 5, 6, and 8.

VAR-DIFF is a feature contrast algorithm and can achieve good performance sometimes, but when the background is very complex, its performance is not very good (for example, in Sequences 2, 4, and 8) since the feature it uses is somewhat simple.

DLCM can achieve a good performance in most of the sequences, but in Sequence 8, its performance is poor.

The proposed algorithm can achieve a good detection performance in all of the eight sequences. Its performance is always at the forefront, and there is no large fluctuation.

C. Tests Against Random Noise

Random noise is an important factor, which makes the detection performance decline. Fig. 6 gives the performances of the proposed algorithm under different levels of random noise using the seven real IR sequences, and zero-mean Gaussian white noises with variances 1–5 are added. It can be seen that the performance of the proposed algorithm is usually stable or only decreases slightly with noise, which confirms the robustness of the proposed algorithm against noise.

V. Conclusion

In this letter, a new nested window is first proposed, which can investigate the characteristics of a local area better. Then, the local gray contrast of the inner and outer windows is chosen as their features, and the RD LFC is calculated between them. In particular, the closest mean principle is adopted to select the benchmark, so that the target will not be drowned by its neighboring high brightness background. Finally, a simple but useful weighting function is proposed to further suppress clutter residuals. Experiments show that the proposed algorithm can achieve good detection performance. In comparison to some existing state-of-the-art algorithms, its detection rate and false alarm rate are better and are robust against noise.

References

[1] Y. Bi, J. Chen, H. Sun, and X. Bai, "Fast detection of distant, infrared targets in a single image using multiorder directional derivatives," *IEEE Trans. Aerosp. Electron. Syst.*, vol. 56, no. 3, pp. 2422–2436, Jun. 2020.

[2] X. Shao, H. Fan, G. Lu, and J. Xu, "An improved infrared dim and small target detection algorithm based on the contrast mechanism of human visual system," *Infr. Phys. Technol.*, vol. 55, no. 5, pp. 403–408, Sep. 2012.

[3] X. Wang, G. Lv, and L. Xu, "Infrared dim target detection based on visual attention," *Infr. Phys. Technol.*, vol. 55, no. 6, pp. 513–521, Nov. 2012.

[4] J. Han, Y. Ma, J. Huang, X. Mei, and J. Ma, "An infrared small target detecting algorithm based on human visual system," *IEEE Geosci. Remote Sens. Lett.*, vol. 13, no. 3, pp. 452–456, Mar. 2016.

[5] Y. Wei, X. You, and H. Li, "Multiscale patch-based contrast measure for small infrared target detection," *Pattern Recognit.*, vol. 58, pp. 216–226, Oct. 2016.

[6] C. L. P. Chen, H. Li, Y. Wei, T. Xia, and Y. Y. Tang, "A local contrast method for small infrared target detection," *IEEE Trans. Geosci. Remote Sens.*, vol. 52, no. 1, pp. 574–581, Jan. 2014.

[7] J. Han, Y. Ma, B. Zhou, F. Fan, K. Liang, and Y. Fang, "A robust infrared small target detection algorithm based on human visual system," *IEEE Geosci. Remote Sens. Lett.*, vol. 11, no. 12, pp. 2168–2172, Dec. 2014.

[8] Y. Qin and B. Li, "Effective infrared small target detection utilizing a novel local contrast method," *IEEE Geosci. Remote Sens. Lett.*, vol. 13, no. 12, pp. 1890–1894, Dec. 2016.

[9] J. Han, K. Liang, B. Zhou, X. Zhu, J. Zhao, and L. Zhao, "Infrared small target detection utilizing the multiscale relative local contrast measure," *IEEE Geosci. Remote Sens. Lett.*, vol. 15, no. 4, pp. 612–616, Apr. 2018.

[10] J. Han, S. Liu, G. Qin, Q. Zhao, H. Zhang, and N. Li, "A local contrast method combined with adaptive background estimation for infrared small target detection," *IEEE Geosci. Remote Sens. Lett.*, vol. 16, no. 9, pp. 1442–1446, Sep. 2019.

[11] X. Guan, Z. Peng, S. Huang, and Y. Chen, "Gaussian scale-space enhanced local contrast measure for small infrared target detection," *IEEE Geosci. Remote Sens. Lett.*, vol. 17, no. 2, pp. 327–331, Feb. 2020.

[12] M. Nasiri and S. Chehresa, "Infrared small target enhancement based on variance difference," *Infr. Phys. Technol.*, vol. 82, pp. 107–119, May 2017.

[13] B. Xiong, X. Huang, and M. Wang, "Local gradient field feature contrast measure for infrared small target detection," *IEEE Geosci. Remote Sens. Lett.*, vol. 18, no. 3, pp. 553–557, Mar. 2021.

[14] H. Deng, X. Sun, M. Liu, C. Ye, and X. Zhou, "Entropy-based window selection for detecting dim and small infrared targets," *Pattern Recognit.*, vol. 61, pp. 66–77, Jan. 2017.

[15] P. Du and A. Hamdulla, "Infrared small target detection using homogeneity-weighted local contrast measure," *IEEE Geosci. Remote Sens. Lett.*, vol. 17, no. 3, pp. 514–518, Mar. 2020.

[16] S. Moradi, P. Moallem, and M. F. Sabahi, "Scale-space point spread function based framework to boost infrared target detection algorithms," *Infr. Phys. Technol.*, vol. 77, pp. 27–34, Jul. 2016.

[17] S. D. Pan *et al.*, "Infrared small target detection based on double-layer local contrast measure," *Acta Photonica Sinica*, vol. 49, no. 1, pp. 184–192, 2020.

Authorized licensed use limited to: XIDIAN UNIVERSITY. Downloaded on August 13,2026 at 11:09:15 UTC from IEEE Xplore. Restrictions apply.